HYBRID COMPLETE COVERAGE PATH PLANNING ALGORITHM FOR SUSPENDED MOWER
/
悬挂式割草机混合全覆盖路径规划算法

Kai RONG, Yi NIU, Ruixue LI, Bolong WANG, Wei LIU, Haoxuan HONG and Guohai ZHANG
Collage of Agricultural Engineering and Food Science, Shandong University of Technology, Zibo, China
Corresponding author: Guohai ZHANG; Tel: +86 15965534882; E-mail: guohaizhang@sdut.edu.cn
DOI: https://doi.org/10.35633/inmateh-77-77

Keywords: *suspended mower; complete coverage path planning; hybrid A* algorithm; Bezier curve; path smoothing; agricultural automation; mowing operations*

ABSTRACT
This paper proposes a Hybrid Complete Coverage Path Planning (HCCPP) algorithm to enhance the efficiency and smoothness of suspended mowers operating in convex polygonal fields. Combining straight-in, nested, and outward-spiral strategies, it optimizes internal and boundary coverage while using Hybrid A and Bézier curves for smooth transitions. The simulation experiment uses a suspended lawn mower (Dongfanghong LX804 rear lawn mower) as the test platform, with parameters: dimensions of 6.50 m × 2.17 m × 2.87 m, working width of 2.5 m, minimum turning radius of 6.2 m, and minimum row spacing of 12.5 m. The simulation experiment of running 5 times for each of the 3 plots shows that HCCPP achieves >99.7% coverage, <5.4% overlap, 4–9% shorter paths, and lower curvature variation, outperforming traditional methods and offering an efficient solution for autonomous agricultural path planning.*

摘要
*本文提出一种混合全覆盖路径规划算法（HCCPP），用于提升悬挂式割草机在凸多边形地块的作业效率与路径平滑性。该方法结合直入、嵌套与外螺旋策略，优化内部与边界区域覆盖，并采用混合 A*与贝塞尔曲线实现平滑过渡。仿真实验以悬挂式割草机（东方红 LX804 后置割草机）为试验平台，参数：尺寸 6.50m×2.17m×2.87m，工作宽度 2.5m，最小转弯半径 6.2m，最小行距 12.5m。对 3 个地块中的每一个进行 5 次运行的仿真实验表明，HCCPP 在多种地块上实现覆盖率超 99.7%，重复率低于 5.4%，路径长度缩短 4%-9%，曲率波动小，优于传统方法，为农机自主路径规划提供高效方案。*

INTRODUCTION
Agricultural mechanization is an important way to improve agricultural production efficiency and reduce labor intensity. As a common agricultural machinery, suspended mower is widely used in forage harvesting, lawn mowing and other fields due to its flexible adaptability with power equipment such as tractors. With the development of intelligent agriculture, it is evolving from manual operation to semi-autonomous and fully autonomous modes. Path planning technology, being a core component, directly determines the efficiency, accuracy, and safety of operations. It is worth noting that the development of agricultural autonomous systems is a complex process that requires the integration of multiple specialized and interrelated subsystems, including path planning, path tracking, localization, and perception systems. This paper will focus on the path planning subsystem.

In agriculture, path-planning tasks are categorized into global path planning and local path planning *(Vagale, Oucheikh et al., 2021)*. Among them, global path planning is path planning based on complete prior information when the operation environment is known, generally in agricultural machinery pre-operation planning *(Li, Huang et al., 2022)*. Local path planning is a real-time path planning that uses sensors to sense environmental information in the work area in agricultural machinery operations *(Ren, Chen et al., 2020, Chen, Gong et al., 2023)*. Complete Coverage Path Planning *(CCPP)* is a global path planning, which refers to planning one or more continuous paths within a given operation area, so that agricultural machinery can cover the entire operational area without omissions and with minimal overlap. Efficient path planning can reduce inefficient driving, reduce energy consumption and time, improve mowing quality, and is of great significance to improve agricultural mechanization level and reduce cost *(Mier, Valente et al., 2022)*.

CCPP process includes two core parts: turn-path planning and traversal-path planning. Turning path planning mainly solves the problem of connecting between working paths. Common methods include semicircle, bow, pear and fishtail turns.

Studies have shown that: for rectangular and trapezoidal fields, bow and pear turns can significantly improve agricultural efficiency *(Jing-fa, Jing et al., 2020)*; strategies based on right-angle turns and fishtail

turns can effectively optimize the outermost and inner corner paths of farmland and improve coverage *(Cheng-ming, Chen-wen et al., 2021)*; dynamic head-turning methods designed for four-wheeled vehicles (using asymmetric backcutting technology) minimize path length and operation time *(He, Bao et al., 2023)*. Bow and pear turns can improve work efficiency by about 15% - 20%, while right-angle and fishtail turns strategies can increase coverage by about 10% - 15%. The dynamic heading turning method uses asymmetric back cutting technology, which can reduce path length and work time by about 20% - 25%. Different turning methods have different distances and application scenarios, but the existing research lacks adaptive turning models that can automatically match the needs of suspended mowers.

The common methods of traversal path planning include reciprocating, spiral, nested and partition. For example, Liu uses reciprocating ergodicity combined with improved ant colony algorithm to improve the adaptability of harvester to unloading position while reducing soil compaction *(Ming-jie, 2021)*. Zhou et al. constructed an environmental model by grid method, and combined with the edge inner spiral algorithm to increase the coverage rate of cleaning robots to 99.3% and reduce the repetition rate to 1.1% *(Xin-yuan, Ling et al., 2021)*. Yang divided sub-regions based on farmland grid, and optimized the traversal order by nested traversal and adaptive genetic algorithm to reduce the path length *(Jie, 2018)*. The current ergodic path research faces challenges such as high complexity, variability and difficulty in implementation. Simple and efficient connection strategies are urgently needed.

Current CCPP research focuses on developing reciprocating or spiraling coverage schemes, but a single approach is difficult to balance coverage integrity and path efficiency over complex terrain *(Höffmann, Patel et al., 2023)*. By linking different coverage modes (such as spiral and reciprocating), hybrid planning methods can customize the path according to the turning radius of agricultural machinery, and optimize fuel and time efficiency while ensuring complete coverage. However, traditional joining methods rely on geometric rules or simple curve fitting, and have three limitations: (1) direct joining leads to abrupt curvature change and increases mechanical wear; (2) the preset path lacks dynamic adjustment ability and is easy to produce coverage gaps; and (3) it is difficult to satisfy multiple constraints of seamless coverage, path minimization and motion smoothing simultaneously. In this paper, hybrid A* algorithm and third-order Bezier curve are introduced to optimize the joint path. Hybrid A* algorithm combines discrete graph search with continuous kinematic constraints to generate feasible paths satisfying turning radius constraints in high-dimensional space, especially for narrow transition regions *(Yang, Pan et al., 2024)*. On this basis, a third-order Bézier curve, with its strong local shape-control capabilities, is used to smooth and optimize the search-generated path, ensuring continuous curvature and keeping the maximum curvature below the upper limit allowed by agricultural machinery dynamics. This significantly enhances driving smoothness and energy efficiency *(Kong, Liu et al., 2024)*. The combination of these two methods achieves a unified balance between global optimality and local smoothness.

The purpose of this study is to propose a hybrid planning method, which combines lawn terrain characteristics and mower operation parameters into a complete coverage path planning system to optimize the path planning model of suspended mower operation scenarios. The specific objectives of this study are: (1) improve the traversal algorithm, and propose a complete coverage path planning algorithm model of "straight-in, minimum-row-spacing nesting, spiral-out"; (2) propose a hybrid complete coverage path planning algorithm for suspended mower operation scenarios by combining hybrid A* algorithm with Bezier curve optimization nested path and outer spiral path; (3) evaluate the system performance through simulation and comparison experiments.

MATERIALS AND METHODS

Algorithm flow

In order to optimize the traverse path of working rows, a path planning algorithm is proposed, which takes the minimum row spacing as the priority. Based on the working row connection path model and traversal path model, a novel hybrid complete coverage path algorithm is proposed, which innovatively combines cross-row nesting and outer spiral methods.

The algorithm flow is as follows: (1) Get plot data and farm machinery operation parameters. (2) Calculate the parameters of hybrid complete coverage path planning algorithm. (3) Generate outer spiral path boundaries and nested path boundaries. (4) Nested paths are generated by minimum row spacing nesting algorithm and pear-shaped and bow-shaped turn models, and outer spiral paths are generated by outer spiral path algorithm and corner turn models. (5) Integrate the outer spiral and nested paths, optimize the connecting path, and generate the complete coverage path.

Optimal coverage path planning meets the core requirements of complete coverage area, reduced number of turns, and shorter working paths *(Lin and Huang, 2021, Chakraborty, Elangovan et al., 2022, Höffmann, Patel et al., 2024)*. According to the characteristics of lawn environment, the following assumptions were made to simplify the model *(Cao, Guo et al., 2023)*: (1) Single agricultural machinery operation. (2) The operation plot is level and free of internal obstacles. (3) The fields are assumed to be regular convex polygons. (4) Farm machinery runs smoothly at a constant speed. (5) Agricultural machinery enters and exits the plot only through specified entrances and exits.

An Improved Nesting Method Integrating Minimum Row Spacing Method

For large farm machinery such as suspended mowers, which has narrow working width but large minimum turning radius, bow turning is often selected as traversal path planning scheme. A path optimization algorithm based on minimum row spacing nesting is proposed in this paper. The longest boundary is selected as the reference path, and the working rows are divided according to the working width of agricultural machinery.

The minimum row spacing $(D_{Min}[m])$ is not a fixed value and needs to be dynamically calculated in combination with the mechanical characteristics of agricultural machinery and operation requirements. The core constraints include: operation width $(b[m])$, mechanical turning radius $(R_{Min}[m])$ and plot slope $(\alpha[°])$. In order to prevent missed cuts due to positioning errors, it is also necessary to introduce an overlap ratio coefficient (k), usually reserving 5% - 20% overlap ratio. The minimum row spacing is the maximum of the constraints above, i.e.:

$$D_{Min} = max\{kb, 2R_{Min}, f(\alpha)\} \tag{1}$$

Typically, $0.8 \leq k \leq 0.95$, $f(\alpha)$ is the slope correction function. The formula for calculating the minimum number of cross rows (n) and the distance between rows (W) is as follows:

$$n = \left\lceil \frac{D_{Min}}{b} \right\rceil \tag{2}$$

$$W = nb \tag{3}$$

where the symbol ⌈ ⌉ indicates rounding up.

The total number of working rows N is calculated as:

$$N = \left\lceil \frac{L}{b} \right\rceil \tag{4}$$

where $L[m]$ is the width of the work area in the direction perpendicular to the reference path, and the value is the maximum distance between two boundary points of the area in that direction.

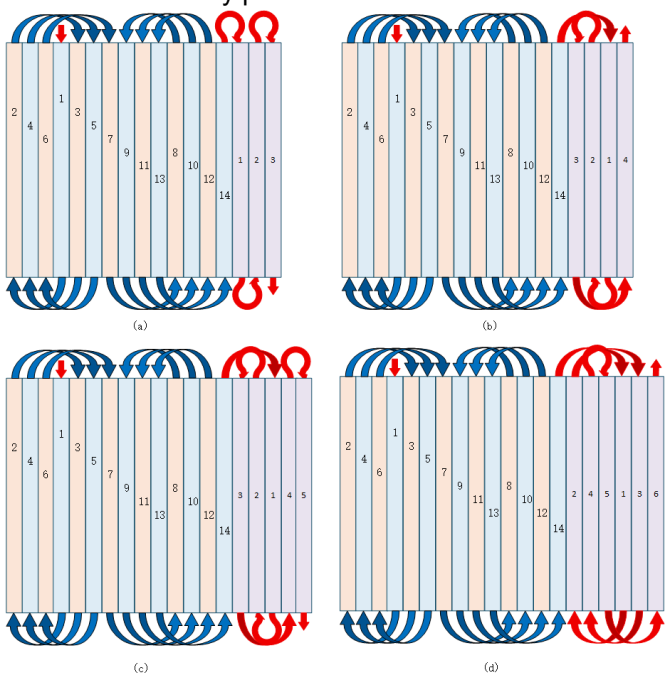

Fig. 1 - Schematic diagram of complete coverage path planning using minimum row spacing nesting method in different cases

(a) When n=3, 1Cn, the planning result of the covering path. (b) When n=3, C=n+1, the planning result of the covering path. (c) When n=3, C=2n-1, the planning result of the covering path. (d) When n=3, C=2n, the planning result of the covering path.

The nesting method based on a minimum spacing of 3 working rows is shown in Figure 1. According to this method, $(2n+1)$ working rows are needed to realize complete coverage. When m groups of paths are executed using the minimum spacing, the total number of working rows becomes $(2nm+m)$. In this model, with a minimum of three spanning rows, 14 working rows are required to complete two nested paths. In this mode, the number of nested path groups (m) with n rows can be calculated as follows:

$$m = \left\lfloor \frac{N}{2n+1} \right\rfloor \quad (5)$$

where the symbol ⌊ ⌋ indicates rounding down. The number of remaining working rows (C) is then calculated as:

$$C = N - M(2n+1) \quad (6)$$

To facilitate the connection between the nested operation and the outer spiral method, the terminal working row should be set as the boundary row. Under the left-starting scheme, the $(n+1)$ row (counting from left to right) is defined as the starting row. The regular characteristics are analyzed as follows:

(1) When $1 \le C \le n$, add C pear turns, as shown in Figure 1(a).

(2) When $n < C < 2n$, planning requires 2 arcuate turns with span (n) and $(C-2)$ pear turns, as shown in Figures 1(b) and 1(c).

(3) When $C = 2n$, planning requires 2 arcuate turns with span $(n+1)$, 3 arcuate turns with span (n) and 1 pear turn, as shown in Figure 1(d).

This method simplifies the connection path into two basic forms: bow turns (when the number of working rows is $(2nm+m)$, with crossing spans of n and $(n+1)$, respectively) and three types of turning paths that incorporate pear turns. Research has shown that traditional bow turns can be replaced by semi-circular turns with larger turning radii (specifically $\frac{nb}{2}$ and $\frac{(n+1)b}{2}$, where $\frac{nb}{2} > R_{Min}$), thereby further streamlining and unifying the turning-path types.

Calculation of outer spiral overburden

In the mowing operation scenario shown in Figure 2, the combination of outer spiral method and corner turning along the edge area of the ground is adopted. The coverage width $(f[m])$ shall be greater than or equal to the turning width $(d[m])$ to ensure the operation efficiency. The optimal sequence of the working rows is determined first by nesting at minimum row spacing, and then by outer spiraling at overlay (F).

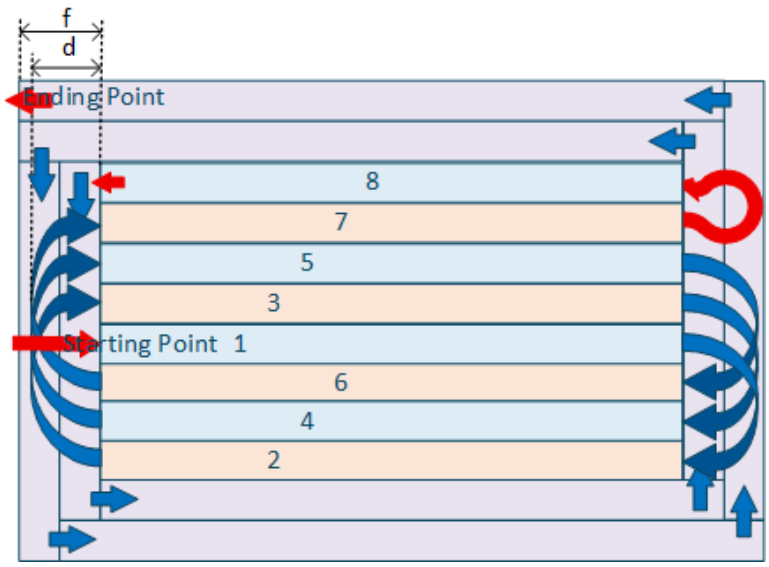

Fig. 2 - Schematic diagram of minimum row spacing nesting and outer spiral method complete coverage

Bow-shaped turns are primarily used for path connections when the spacing between parallel working rows exceeds twice the minimum turning radius $(W > 2R_{Min})$. When the nested-method connection path uses bow turns (as shown in Figs. 3a and 3b), the number of outer-spiral coverage layers F is calculated using Eq.(7). When the connection path uses a semicircular turn, the number of outer-spiral coverage layers F is calculated using Eq. (8).

$$F = \left\lceil \frac{(W-R_{Min})\cos\alpha + R_{Min}}{b} \right\rceil \quad (7)$$

$$F = \left\lceil \frac{(W-R)\cos\alpha + R}{b} \right\rceil \quad (8)$$

where $\alpha[rad]$ is the angle between the current working row and the boundary of the plot. The working path length for this type of turn consists of two components: one is a semicircular turning path with radius R, and a straight path segment. Due to the fixed turning radius (R), the length of the straight segment directly determines the row spacing required for cross-row operations.

Pear-shaped turns are mainly suitable when the spacing between parallel working rows is less than twice the minimum turning radius $(W < 2R_{\min})$. This turning technique consists of three consecutive arc segments, with the curvatures of the first and last arc segments corresponding to angles β(rad) and γ(rad), respectively. A larger curvature value results in smaller spacing between working rows, whereas a smaller curvature value increases the spacing. However, the spacing must always satisfy the condition $W < 2R_{\min}$. When the connection path adopts pear-shaped turns (as shown in Figs. 3c and 3d), the number of coverage layers in the outer spiral method F is calculated using Eq. (9):

$$F = \left\lceil \frac{(4R_{Min}\sin\gamma + W\cot\alpha)\sin\alpha}{2b} + \frac{R_{Min}}{b} \right\rceil \quad (9)$$

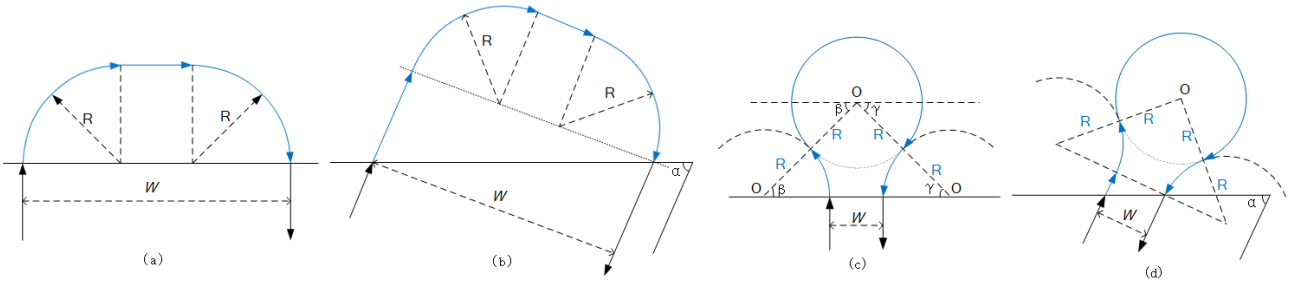

Fig. 3 - Turning methods

(a) Bow turn with parcel boundary perpendicular to the working path;
(b) Bow turn with parcel boundary not perpendicular to the working path;
(c) Pear turn with parcel boundary perpendicular to the working path;
(d) Pear turn with parcel boundary not perpendicular to the working path

Constraints on Joining Path

In the improved nesting method based on a minimum of three spanning rows, the nested path ends on the same side as the starting point when the remaining number of rows C is even, and ending on the opposite side of the starting point when C is odd. According to the counterclockwise outer spiral operation rule, the theoretical initial loop of outer spiral can be deduced. Then a local search target area is constructed with the outer spiral starting point as the center. The size of this area should be determined according to the turning radius of the agricultural machinery, the working width and the required smoothness *(Vahdanjoo, Gislum et al., 2024)*. The hybrid A* algorithm automatically searches for connecting paths to ensure continuity of coverage.

A joining path must satisfy three core constraints simultaneously:

(1) Geometric constraints: The path must lie entirely within the transition region between the outer-spiral boundary and the nested boundary and must not exceed the parcel boundary. The turning radius must be greater than or equal to the minimum turning radius.

(2) Coverage constraints: The joining path must fully cover the theoretical starting loop. The lateral deviation must be ≤ 0.5 times the working width to avoid missed coverage or redundant coverage.

(3) Dynamic constraints: The path must maintain continuity, with a maximum curvature $\leq 0.33m^{-1}$ and a rate of directional change $\leq 15^{\circ}/m$, in order to reduce tractor steering energy consumption and mechanical wear.

Implementation of Hybrid A * Algorithm

1. State space definition:

A three-dimensional state vector (x, y, θ) is used to describe the position and orientation of the agricultural machine, where (x, y) are planar coordinates and θ is the heading angle (the angle relative to the x-axis). State transitions must comply with the kinematic constraints of the tractor.

2. Heuristic function design:

In the heuristic function $f(n) = g(n) + h(n)$, $g(n)$ is the actual cost (including path length and turning-penalty terms) from the nested endpoint to the current node, $h(n)$ is the estimated cost from the current node to the outer spiral start point.

A Euclidean distance with directional weighting is used:

$$h(n) = \alpha \cdot \sqrt{(x_g - x_n)^2 + (y_g - y_n)^2} + \beta \cdot |\theta_g - \theta_n| \quad (10)$$

where, $\alpha = 0.6$ and $\beta = 0.4$ are weighing coefficients, weight $\alpha > \beta$ giving higher priority to distance cost. (x_g, y_g, θ_g) is the target state corresponding to the starting point of the outer spiral (where θ_g is the initial tangent direction of the outer spiral).

3. Node expansion and pruning:

A dynamic neighborhood-expansion strategy is adopted. A 14-neighborhood search is used in unobstructed areas to accelerate convergence, while an 8-neighborhood search is applied near boundaries to ensure accuracy. Nodes exhibiting excessive curvature are pruned, and, within each grid cell, the three states with the lowest cost are retained.

4. Path extraction: After the search reaches the starting point of the outer spiral, an initial connecting path consisting of approximately 15–20 key nodes is generated by tracing back through the parent nodes.

Third-order Bezier curve smoothing

1. Control point selection:

Four key control points are extracted from the Hybrid A* generated path: P_0 (nested-path endpoint), P_1 (direction feature point), P_2 (transition feature point), P_3 (outer-spiral starting point). Points P_1 and P_2 are optimized using a least-squares fitting approach. By sampling the intermediate nodes of the Hybrid A* path, the mean squared error between the Bézier curve and the sample points is minimized (≤ 0.5 m), ensuring that the smoothed curve does not deviate from the original optimized path direction.

2. Curve Generation and Curvature Constraints:

The third-order Bézier curve is defined as:

$$B(t) = (1-t)^3 P_0 + 3t(1-t)^2 P_1 + 3t^2(1-t)P_2 + t^3 P_3 \quad t \in [0,1] \quad (11)$$

Derivation of the curve yields the first derivative $B'(t)$ and the second derivative $B''(t)$, and by adjusting the coordinates of P_1 and P_2, ensures that the curvature $\gamma(t) = |B'(t) \times B''(t)|/|B'(t)|^3$ satisfies $\gamma(t) \leq 0.33m^{-1}$.

3. Coverage accuracy correction:

Final correction is performed by offsetting control point P_1 to ensure complete coverage of the bridging segment between the nested path and the outer spiral.

Simulation test design

Three typical plots on the south lawn of the Yifu Library at Shandong University of Technology were selected as test sites and labeled Parcel No. 1, No. 2, and No. 3. The basis for parcel selection was as follows: Parcel 1 is a regular rectangle representing simple, flat terrain and was used to evaluate the basic performance of the algorithm under ideal conditions. Parcels 2 and 3 are irregular polygons with convex corners, simulating common irregular-field scenarios and focusing on verifying the algorithm's adaptability to complex boundaries. The boundary coordinates of all plots were collected using RTK differential positioning with a sampling interval of 5 m, and vector models were constructed after boundary optimization using the Douglas-Peucker algorithm (Kai, Yin-shan et al., 2022). This algorithm enables polygon fitting by simplifying redundant linear features while preserving the original geometric structure of the boundary.

The experiment used a suspended mower (Dongfanghong LX804 rear-mounted mower) as the test platform. Its parameters are as follows: overall dimensions of 6.50 m × 2.17 m × 2.87 m, a working width of 2.5 m, a minimum turning radius of 6.2 m, and a minimum row spacing of 12.5 m. The simulation environment consisted of a Windows 11 operating system (Intel Core i5-13400, 2.5 GHz, 32 GB RAM). MATLAB R2024a was used for algorithm simulation, while path generation and analysis were performed using custom MATLAB scripts.

The comparison framework was designed as follows:

1. Control group 1 (minimum row-spacing nesting method):

The optimal nesting algorithm proposed in Section 4.1 of this paper was used as the benchmark to evaluate the improvement provided by the "outer-spiral boundary coverage" module. Its parameter settings were consistent with HCCPP, with a minimum row spacing of $D_{\min} = 12.5$ m and a spanning-row number of $n = 5$.

2. Control group 2 (outer-spiral + reciprocating hybrid):

The traditional hybrid strategy combining inner reciprocating paths with an outer spiral boundary was used to assess the effectiveness of HCCPP in optimizing transfer paths in non-working areas and reducing deadhead travel distance. The reciprocating section adopted pear-shaped turns, while the spiral layers were kept consistent with HCCPP.

3. Experimental group (HCCPP algorithm proposed in this paper):

The proposed "straight-in → minimum-row-spacing nesting → spiral-out" framework was employed. The connecting path was generated using the Hybrid A* algorithm followed by third-order Bézier curve optimization, with curvature constrained to $\leq 0.33m^{-1}$.

Uniform operating constraints:

Working width $b = 2.5$ m; overlap ratio $k = 0.9$; minimum turning radius $R_{\min} = 6.2$ m; straight-line travel speed $V_s = 1.5$ m/s; turning speed $V_t = 0.8$ m/s.

Each method was executed independently five times on each plot, and the averaged results were reported to reduce random error interference.

Evaluation index

1. Coverage rate: the ratio of the area effectively covered by the planned path to the total field area. The ideal value is 100%. Values below 99% indicate missed coverage.

2. Duplicate coverage: refers to the ratio of the total area actually traversed by the planned path to the area of the plot, reflecting route redundancy. Lower values indicate better performance.

3. Total path length: the total distance of the planned path (including both working rows and turning segments), measured in meters. This metric directly affects operation time and energy consumption.

4. Non-working path ratio: the ratio of the length of non-working travel (turning segments) to the total path length. A lower ratio indicates higher path efficiency.

5. Number of turns: the total number of turns in the path (including bow turns, pear turns, and corner turns). Fewer turns correspond to reduced mechanical wear and lower energy consumption.

6. Path smoothness: quantified by the standard deviation of curvature fluctuations along the path. Lower values indicate smoother, more stable trajectories.

RESULTS

Results analysis

The coverage and duplicate-coverage results of the three methods across the three test plots are presented in Table 1. The HCCPP method achieved a coverage rate exceeding 99.7% in all plots. In contrast, Control Group 1 exhibited missed coverage ranging from 1.4% to 2.2% in Plots 2 and 3, while Control Group 2 suffered substantial missed coverage (98.5%–99.5%) due to gaps in the joining region. The duplicate-coverage rate of HCCPP ranged from 3.5% to 5.4%, significantly lower than that of Control Group 1 (5.2% - 8.7%) and Control Group 2 (6.8% - 9.5%).

Table 1

Comparison of Coverage Performance (mean ± standard deviation)

Plot number	Group	Coverage rate [%]	Duplicate coverage rate [%]
1	Control Group 1	99.8 ± 0.15	5.2 ± 0.28
	Control Group 2	99.5 ± 0.22	6.8 ± 0.35
	Experimental Group	99.9 ± 0.08	3.5 ± 0.18
2	Control Group 1	98.6 ± 0.31	7.5 ± 0.42
	Control Group 2	99.2 ± 0.25	8.3 ± 0.39
	Experimental Group	99.8 ± 0.12	4.8 ± 0.22
3	Control Group 1	97.8 ± 0.45	8.7 ± 0.51
	Control Group 2	98.5 ± 0.38	9.5 ± 0.48
	Experimental Group	99.7 ± 0.18	5.4 ± 0.26

The total path length, proportion of non-working paths, and number of turns for the three methods are summarized in Table 2. The total path length of the HCCPP method was 4% - 6% shorter than that of Control Group 1 and 7% - 9% shorter than that of Control Group 2. The proportion of non-working paths ranged from 13.2% to 17.8%, which was lower than that of Control Group 1 (18.5% - 23.5%) and Control Group 2 (21% - 26.2%). In addition, the number of turns in HCCPP was 15% - 19.4% lower than in Control Group 1 and 31.5% - 34.6% lower than in Control Group 2.

Table 2

Efficiency performance comparison (mean ± standard deviation)

Plot number	Group	Total path length[m]	Proportion of non-working paths [%]	Number of turns
1	Control Group 1	712.83 ± 8.45	18.5 ± 1.2	20 ± 1.8
	Control Group 2	737.26 ± 10.32	21.0 ± 1.5	26 ± 2.1
	Experimental Group	682.47 ± 5.23	13.2 ± 0.8	17 ± 1.2
2	Control Group 1	781.39 ± 12.67	22.0 ± 1.8	32 ± 2.4
	Control Group 2	812.72 ± 15.84	24.8 ± 2.1	38 ± 2.9
	Experimental Group	743.18 ± 7.35	16.5 ± 1.1	26 ± 1.6
3	Control Group 1	851.64 ± 18.23	23.5 ± 2.2	36 ± 3.1
	Control Group 2	883.93 ± 20.15	26.2 ± 2.5	43 ± 3.5
	Experimental Group	801.27 ± 9.87	17.8 ± 1.4	29 ± 1.9

The standard deviation (SD) of curvature fluctuation for HCCPP was approximately 0.1 m^{-1}, which is lower than that of Control Group 1 (0.16 m^{-1}) and Control Group 2 (0.20 m^{-1}). The Bézier curve maintained curvature within 0.32 m^{-1}, satisfying the dynamic constraints.

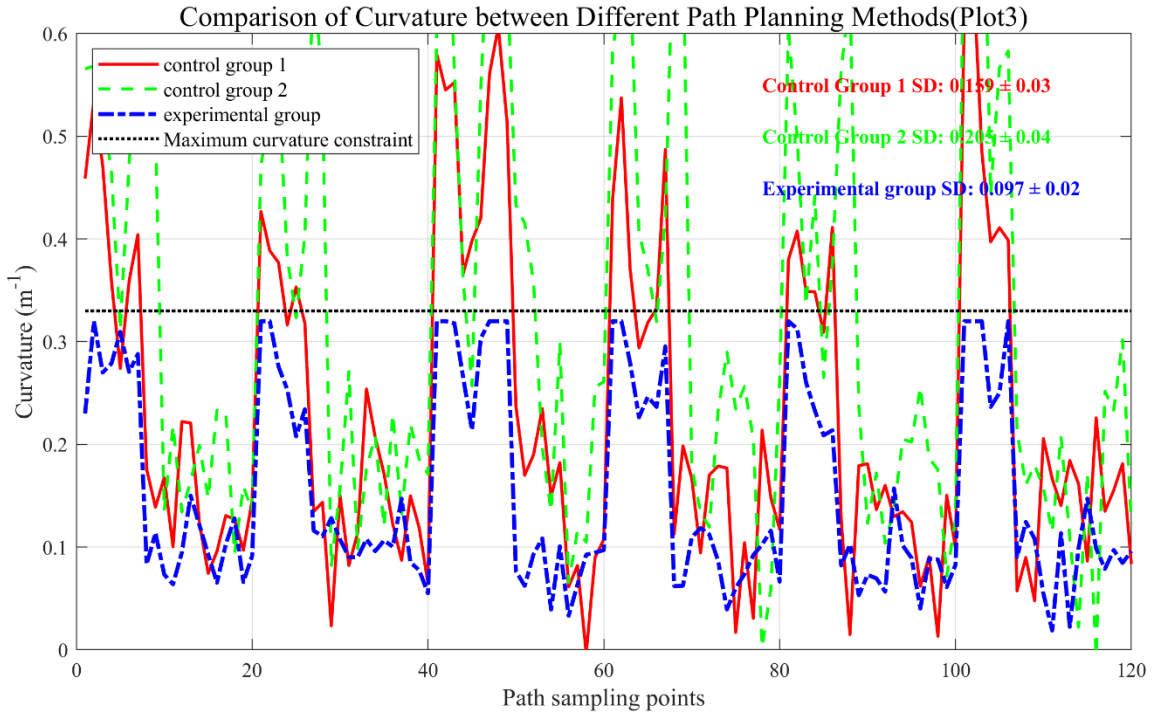

Fig. 4 - Comparison of Path Smoothness

Parameter sensitivity analysis

After verifying the benchmark performance of the HCCPP algorithm, a sensitivity analysis of key operational parameters was conducted to evaluate the robustness of the algorithm and its response to parameter variations. The analysis focuses on two core parameters: the overlap ratio k and the minimum row spacing D_{Min}. Together, these parameters determine the effective coverage width and turning mode of the planned path, and they are critical for balancing working quality and operational efficiency.

Analysis shows that the overlap ratio k is a highly sensitive parameter. When its value deviates from the benchmark setting $(k = 0.9)$, the algorithm exhibits a clear performance trade-off. When k falls below 0.85, the total path length becomes the shortest; however, simulation results show a substantial increase in the risk of missed coverage, and overall coverage may drop below 98%. This is primarily due to reduced tolerance for machinery-positioning errors and steering drift. Conversely, when k exceeds 0.93, coverage can still remain close to 100%, but the duplicate coverage rate increases almost linearly to an unacceptable level (>10%). This leads to path redundancy, reduced operational efficiency, and potential lawn damage caused by repeated compaction. Therefore, a "sweet zone" for the overlap ratio exists - approximately 0.88 - 0.92 - within which the algorithm achieves an optimal balance between high coverage and low duplicate coverage.

The minimum row spacing D_{Min} is a moderately sensitive parameter. In this study, the agricultural machinery parameters were fixed $(R_{Min} = 6.2m, b = 2.5m)$ and D_{Min} was primarily determined by the minimum turning radius $(2R_{Min} = 12.4m)$. This value, in turn, defines the minimum spanning number $n = 5$and the corresponding bow-turning mode. If the effective turning radius increases due to variations in ground-adhesion conditions, both D_{Min} and n will change accordingly. Such changes directly impact the global path structure, particularly by enlarging the turning region and increasing the proportion of non-working paths. It is worth noting that for smaller agricultural machines (with a smaller R_{Min}), D_{Min} may instead be dominated by the product $k * b$. In such cases, even small fluctuations in the overlap ratio k may trigger switching between turning strategies (bow vs. pear turns), thereby significantly increasing parameter sensitivity.

In summary, the strong performance of the HCCPP algorithm demonstrates good stability near the benchmark parameter settings; however, it is particularly sensitive to the overlap ratio k. This analysis provides important guidance for practical deployment: before field application, the optimal local value of k should be identified through small-scale parameter scanning that accounts for the specific positioning accuracy of the agricultural machinery and the operational environment. This ensures that the algorithm can perform reliably under real-world conditions. The sensitivity analysis also indirectly verifies the effectiveness of the nested strategy based on minimum row spacing. While this strategy guarantees the feasibility of path planning through rigid geometric constraints, the ultimate operational and economic benefits depend on fine-tuning key parameters to match the machine and field characteristics.

CONCLUSIONS

(1) To address the challenge of complete-coverage path planning in convex polygon fields, a hybrid navigation path-planning method suitable for suspended mower operations was proposed. Based on actual mowing requirements, a hybrid complete-coverage path-planning algorithm integrating minimum row-spacing nesting was developed.

(2) Simulation experiments on three real-world plots demonstrate that the proposed hybrid algorithm meets the operational requirements of suspended-mower mowing tasks. The method effectively optimizes the working path, significantly shortens the total path length, and reduces the proportion of non-working travel. Following the engineering principle that "path shortening is directly associated with reduced energy consumption," this algorithm is expected to lower fuel consumption in practical applications while minimizing mechanical wear and soil-compaction effects - thus contributing to sustainable agricultural practices. However, these benefits require verification through future empirical field studies.

(3) The proposed complete-coverage path-planning method for suspended mowers is primarily designed for convex polygon plots and exhibits strong generality, making it applicable to convex plots of varying complexity and size. Although validation was conducted on small plots, the number and diversity of test cases were limited by available lawn area and plot complexity. Therefore, further evaluation on a broader range of plot shapes and real-world conditions is necessary to fully assess the method's versatility. The current approach does not consider more complex scenarios such as concave polygon fields, internal obstacles, or dynamic obstacles. Future research may address these limitations by decomposing concave or obstacle-containing plots into multiple convex polygons and by integrating dynamic obstacle-avoidance path-planning algorithms to enhance robustness and adaptability.

REFERENCES

[1] Cao, R., Guo, Y., Zhang, Z., Li, S., Zhang, M., Li, H., & Li, M. (2023). Global path conflict detection algorithm of multiple agricultural machinery cooperation based on topographic map and time window (基于地形图和时间窗口的多农机协同全局路径冲突检测算法). *Computers and Electronics in Agriculture*, Vol. 208, pp. 107773, Beijing/China. https://doi.org/10.1016/j.compag.2023.107773

[2] Chakraborty, S., Elangovan, D., Govindarajan, P. L., ELnaggar, M. F., Alrashed, M. M., & Kamel, S. (2022). A Comprehensive Review of Path Planning for Agricultural Ground Robots. *Sustainability*, Vol. 14(15), pp. 9156, India. https://doi.org/10.3390/su14159156

[3] Chen, B., Gong, L., Yu, C., Du, X., Chen, J., Xie, S., Le, X., Li, Y., & Liu, C. (2023). Workspace decomposition based path planning for fruit-picking robot in complex greenhouse environment (复杂温室环境下基于工作空间分解的水果采摘机器人路径规划). *Computers and Electronics in Agriculture*, Vol. 215, pp. 108353, Shanghai/China. https://doi.org/10.1016/j.compag.2023.108353

[4] Chen, K., Yin, X. S., Li, L. Y., Li, L. C., & Meng, M. J. (2022). Full Coverage Path Planning Method of Agricultural Machinery under Multiple Constraints (多约束情形下的农机全覆盖路径规划方法). *Transactions of the Chinese Society for Agricultural Machinery*, Vol. 53(05), pp. 17-26+43, Shanghai/China.

[5] He, Z., Bao, Y., Yu, Q., Lu, P., He, Y., & Liu, Y. (2023). Dynamic path planning method for headland turning of unmanned agricultural vehicles (无人农业车辆地头转向的动态路径规划方法). *Computers and Electronics in Agriculture*, Vol. 206, pp.107699, Zhejiang/China.

[6] Höffmann, M., Patel, S., & Büskens, C. (2023). Optimal Coverage Path Planning for Agricultural Vehicles with Curvature Constraints. *Agriculture*, Vol. 13(11), pp. 2112, Germany. https://doi.org/10.3390/agriculture13112112

[7] Höffmann, M., Patel, S., & Büskens, C. (2024). Optimal guidance track generation for precision agriculture: A review of coverage path planning techniques. *Journal of Field Robotics,* Vol. 41(3), pp. 823-844, Germany. https://doi.org/10.1002/rob.22286

[8] Kong, F., Liu, B., Han, X., Yi, L., Sun, H., Liu, J., Liu, L., & Lan, Y. (2024). Path Planning Algorithm of Orchard Fertilization Robot Based on Multi-Constrained Bessel Curve (基于多约束贝塞尔曲线的果园施肥机器人路径规划算法). *Agriculture*, Vol. 14(7), pp. 979, Shandong/China.

[9] Li, C. M., Chen, X. W., He, H. M., Du, D. Y., & Wang, W. S. (2021). Coverage operation path planning algorithms for the rape combine harvester in quadrilateral fields (四边形田块下油菜联合收获机全覆盖作业路径规划算法). *Journal of Agricultural Engineering*, Vol. 37(09), pp. 140-148, Hubei/China.

[10] Li, C., Huang, X., Ding, J., Song, K., & Lu, S. (2022). Global path planning based on a bidirectional alternating search A* algorithm for mobile robots (基于双向交替搜索 A*算法的移动机器人全局路径规划). *Computers & Industrial Engineering,* Vol. 168*,* pp. 108123*,* Sichuan/China.

[11] Li, M. J. (2021). Research on path planning and path tracking methods of Intelligent harvester (智能收割机路径规划与跟踪方法研究). *Southeast University*, Jiangsu/China.

[12] Lin, H.-Y., & Huang, Y.-C. (2021). Collaborative Complete Coverage and Path Planning for Multi-Robot Exploration (多机器人探索的协作式完全覆盖与路径规划). *Sensors*, Vol. 21(11), pp. 3709, Taiwan/China. https://doi.org/10.3390/s21113709

[13] Mier, G., Valente, J., & de Bruin, S. (2022). Fields2Cover: An open-source coverage path planning library for unmanned agricultural vehicles. *IEEE Robotics and Automation Letters*, Vol. 8(4), pp. 2166–2172, The Netherlands. https://doi.org/10.48550/ARXIV.2210.07838

[14] Ren, H., Chen, S., Yang, L., & Zhao, Y. (2020). Optimal Path Planning and Speed Control Integration Strategy for UGVs in Static and Dynamic Environments (无人地面车辆在静态和动态环境中的最优路径规划与速度控制集成策略). *IEEE Transactions on Vehicular Technology*, Vol. 69(10), pp. 10619–10629, Beijing/China. https://doi.org/10.1109/tvt.2020.3015582

[15] Vagale, A., Oucheikh, R., Bye, R. T., Osen, O. L., & Fossen, T. I. (2021). Path planning and collision avoidance for autonomous surface vehicles I: a review. *Journal of Marine Science and Technology*, Vol. 26(4), pp. 1292-1306, Norway. https://doi.org/10.1007/s00773-020-00787-6

[16] Vahdanjoo, M., Gislum, R., & Sørensen, C. A. G. (2024). Three-dimensional area coverage planning model for robotic application. *Computers and Electronics in Agriculture*, Vol. 219, p. 108789, Denmark. https://doi.org/10.1016/j.compag.2024.108789

[17] Yang, C., Pan, J., Wei, K., Lu, M., & Jia, S. (2024). A Novel Unmanned Surface Vehicle Path-Planning Algorithm Based on A and Artificial Potential Field in Ocean Currents (一种基于 A*算法和人工势场的新型无人水面艇在海流中的路径规划算法). *Journal of Marine Science and Engineering*, Vol. 12(2), p. 285, Fujian/China. https://doi.org/10.3390/jmse12020285

[18] Ye, J. (2018). Research on agricultural machinery automatic navigation based on wireless sensor networks (基于 WSN 的农机自动导航技术研究). *Southwest Jiaotong University*, Sichuan/China.

[19] Yin, J. F., Li, L. J., Zeng, Z. F., & Tang, T. G. (2020). Optimization of agricultural machinery operation path based on doppler and greedy strategy (基于多普勒与贪心策略的农机作业路径优化研究). *Journal of Chinese Agricultural Mechanization*, Vol. 41(04), pp. 130-137, Hebei/China.

[20] Zhang, X. Y., Zeng, Z. L., & Ma, M. Y. (2021). The Application of Environment Modeling Based on Grid Map in Path Planning of Cleaning Robot (基于栅格地图的环境建模在清洁机器人路径规划中的应用). *Management & Technology of SME*, No. 07, pp. 183-184, Jiangsu/China.